How to cite: Angew. Chem. Int. Ed. 2024, e202406425
doi.org/10.1002/anie.202406425

Hydrogen Storage

Strong Swelling and Symmetrization in Siliceous Zeolites due to Hydrogen Insertion at High Pressure

*Mario Santoro, Jérôme Rouquette, Marco Fabbiani, Francesco di Renzo, Benoît Coasne, Weiwei Dong, Konstantin Glazyrin, and Julien Haines**

Abstract: Hydrogen and helium saturate the 1D pore systems of the high-silica (Si/Al > 30) zeolites Theta-One (TON), and Mobile-Twelve (MTW) at high pressure based on x-ray diffraction, Raman spectroscopy and Monte Carlo simulations. In TON, a strong 22 % volume increase occurs above 5 GPa with a transition from the collapsed $P2_1$ to a symmetrical, swelled $Cmc2_1$ form linked to an increase in H_2 content from 12 H_2/unit cell in the pores to 35 H_2/unit cell in the pores **and in the framework of the material**. No transition and continuous collapse of TON is observed in helium indicating that the mechanism of H_2 insertion is distinct from other fluids. The insertion of hydrogen in the larger pores of MTW results in a strong 11 % volume increase at 4.3 GPa with partial symmetrization followed by a second volume increase of 4.5 % at 7.5 GPa, corresponding to increases in hydrogen content from 43 to 67 and then to 93 H_2/unit cell. Flexible 1D siliceous zeolites have a very high H_2 capacity (1.5 and 1.7 H_2/SiO_2 unit for TON and MTW, respectively) due to H_2 insertion in the pores and the framework, in contrast to other atoms and molecules, thereby providing a mechanism for strong swelling.

The behavior of hydrogen is of fundamental importance for chemistry,[1] physics,[2] planetary science[3] and for energy applications.[4] Confinement in porous materials can lead to novel states of adsorbed nanophases of hydrogen[5] and may also be an option for hydrogen storage. Similar states would only be expected in bulk hydrogen at much lower temperatures and/or much higher pressures. Small pore sizes favor strong densification and the ordering of hydrogen molecules with the reduction in rotational degrees of freedom.[5e] The ortho:para nuclear spin isomer ratio, a critical parameter for hydrogen storage density, is also modified under such confinement conditions.[5e] The use of zeolites, microporous aluminosilicates, can allow for extreme confinement of hydrogen on a sub-nano scale in the pores of these materials, which are typically less than 1 nm. High pressure can be used to obtain very dense confined hydrogen in the pores of these materials. Investigations of hydrogen insertion in the zeolite MFI (Mobile-Five)[5c] with a three-dimensional, elliptical 5.1×5.5 Å diameter, pore system showed that, due to its small size, a much greater amount of hydrogen can enter in the pore system than for other fluids (CO_2,[6] H_2O[7]), except for helium.[8] This results in a much lower compressibility of MFI in hydrogen and stabilization of the zeolite structure up to at least 60 GPa, which is much higher than the pressure at which zeolites become amorphous. A swelling of the unit cell of the siliceous zeolite TON (Theta-One), with a 1D 4.7×5.5 Å elliptical pore system, by close to 6 % was also observed due to filling with hydrogen obtained by the dehydrocoupling of ammonia borane under high temperature, high pressure conditions of 4 GPa and 217 °C.[9] The products of the polymerization of ammonia borane also occupied the pores along with hydrogen.

In contrast to H_2 at high pressure and high temperature, the filling of TON under high pressure at ambient temperature with other fluids, such as Ne,[10] Ar,[10] N_2,[11] O_2[11] and

[*] J. Rouquette, M. Fabbiani, F. di Renzo, J. Haines
ICGM, CNRS, Université de Montpellier, ENSCM,
34293 Montpellier, France
E-mail: julien.haines@umontpellier.fr

M. Santoro
Istituto Nazionale di Ottica,
CNR-INO
50019 Sesto Fiorentino, Italy

M. Santoro
European Laboratory for Non Linear Spectroscopy (LENS),
50019 Sesto Fiorentino, Italy

B. Coasne
Université Grenoble Alpes, CNRS, LIPhy,
38000 Grenoble, France

B. Coasne
Institut Laue Langevin,
F-38042, Grenoble, France

W. Dong, K. Glazyrin
Deutsches Elektronen-Synchrotron DESY,
Notkestr. 85, 22607 Hamburg, Germany

W. Dong
Beijing Synchrotron Radiation Facility,
Institute of High Energy Physics,
Chinese Academy of Sciences,
Beijing, 100049, People's Republic of China

H_2O,[7] reduces the apparent compressibility of the structure due to guest insertion in the pores, but swelling is not observed. In all cases, the high-pressure phase transition from the orthorhombic, $Cmc2_1$ low-pressure phase to the $Pbn2_1$ high-pressure phase is observed as found also in TON with empty pores at close to 0.6 GPa.[12] This transition is linked to partial collapse of the pores. A similar high-pressure, phase transition[13] is also observed in a second siliceous zeolite of interest MTW (Mobil Twelve) with larger 1D 6.9 Å×5.6 Å elliptical pores. Again, pore collapse is involved in the phase transition from the $C2/c$ to the $P2/n$ structures.

In the present study, hydrogen and helium are directly compressed in the pores of TON. In the case of hydrogen, a much greater swelling of the unit cell is observed as compared to any other zeolite-guest system. Such behavior appears to be restricted to hydrogen as continuous compression is observed in helium after initial filling. Hydrogen was also compressed in the larger pores of the zeolite MTW, with again a high degree of swelling, which also showed some metastability with decreasing pressure. These results support promising potential for hydrogen storage.

In the present work, TON was first studied by synchrotron, x-ray diffraction (see SI), using He as a pressure-transmitting medium. Very weak superlattice reflections are observed starting from the third pressure point at 1.16 GPa. These reflections rapidly increase in intensity with increasing pressure and the strongest exhibits relative intensities of close to 10 % at 10.1 GPa, Figure 1. This behavior is similar to that observed when neon[10] is used as a pressure-transmitting medium. This indicates that in these filled systems the high-pressure phase transition from the $Cmc2_1$ to the $Pbn2_1$ form still occurs; however, the distortion linked to pore collapse is much lower than in the case of the compression of empty-pore TON in a non-penetrating pressure-transmitting medium (such as DAPHNE7474[12]), for which the relative intensities of such superlattice reflections are greater than 20 % at similar pressures. Rietveld refinements, Figure S1 and Tables S1–S7, allowed the structure of the framework to be determined below and above the phase transition, Figure S2.

The relative unit cell volumes of TON in He (Figure 2 and Table S1) decrease slightly more than those measured in Ne indicating that He may over a certain pressure range occupy a lower fraction of the pore volume in TON. This may correspond to the same number of guest atoms, but which have a smaller kinetic diameter in the case of He. The relative volumes of TON are similar in both noble gases above 5 GPa. This indicates that globally the behavior of TON in He is very similar to that in Ne[10] with the same high pressure phase transition being observed and only some differences in unit cell volume below 5 GPa.

In spite of the similar kinetic diameters of H_2 (2.89 Å), He (2.60 Å) and Ne (2.75 Å),[14] the high-pressure behavior of TON in H_2 will be shown to be distinct based on the results of the present study described in the following section. Initially, very weak superlattice peaks are present at 1.6 GPa, which increase in intensity at 2.7 GPa. They are, however, much weaker than in He. At the same time, unlike

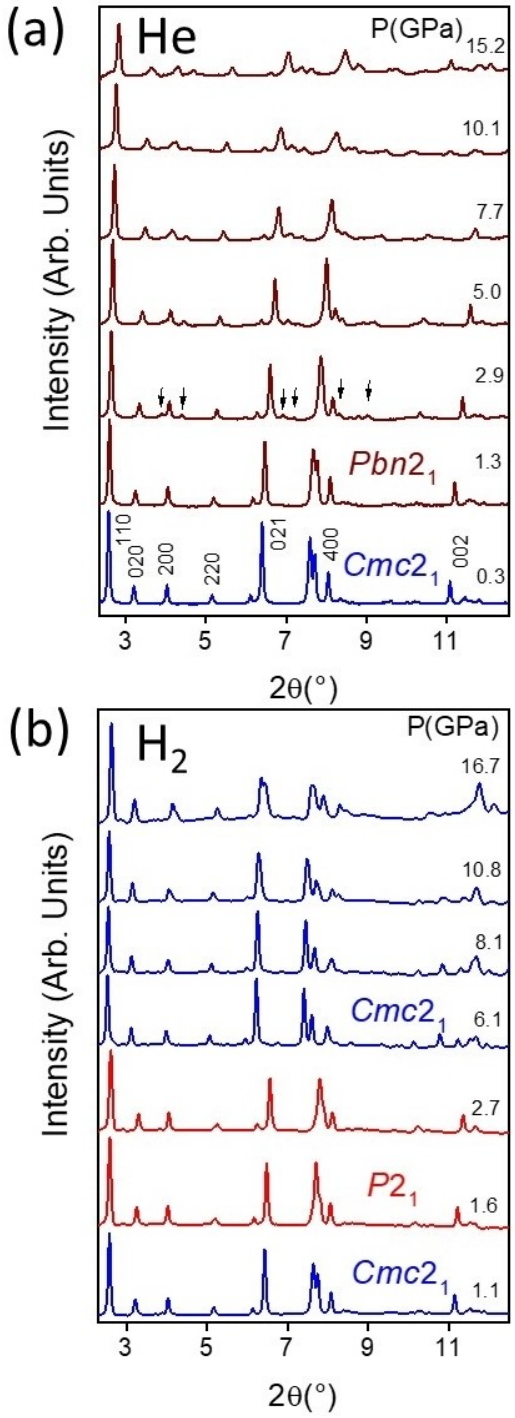

Figure 1. X-ray diffraction patterns of TON in (a) helium and in (b) hydrogen as a function of pressure (λ = 0.4828 Å). Selected reflections of the low-pressure $Cmc2_1$ phase at 0.3 GPa are indexed. Arrows indicate the principal superlattice reflections observed for the $Pbn2_1$ phase in helium.

in He, slight splitting of the $hk0$ and hkl reflections (with non-zero indices) was observed. This indicates a monoclinic distortion of the structure and the reflections could be readily indexed in the monoclinic subgroup $P112_1$ with a γ angle between 90.5 and 91° (Figures 1–2, S3–S4, Tables S1,

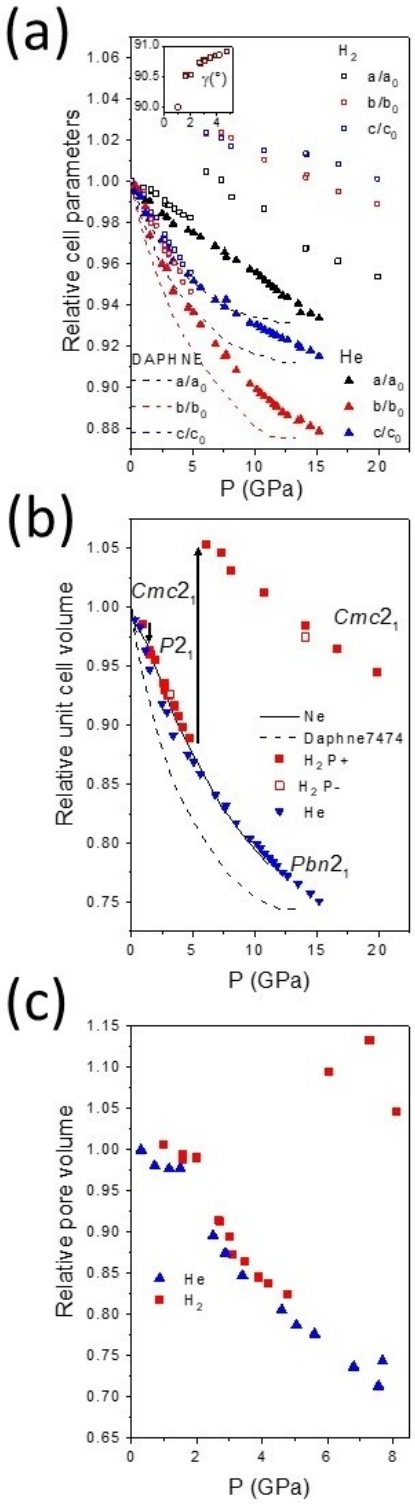

Figure 2. (a) Relative unit cell parameters, (b) relative unit cell volume and (c) relative pore volume of TON in H_2 and He as a function of pressure. Error bars are smaller than the symbol size. Data for TON in DAPHNE7474,[12] Ne[10] and Ar[10] are from previous studies. The monoclinic angle γ for TON in H_2 is given in the inset.

S11–S13). The structure of the framework could also be refined in this space group.

Additionally, the unit cell volume in H_2 is 1–2 % greater than in He. If the filling was proportional to the numerical densities of the bulk fluids,[15] one would expect 50 % more helium than hydrogen in the pores due to the larger size of the freely rotating H_2 molecules. However, if the steric effects limit the occupation to 6 guests per pore[10] as observed in Ne, the larger volume may just be related to the size of the freely rotating H_2 molecules. The present result may also indicate that the rotational state of the H_2 in the pores may be modified. The structure is also less distorted and the pores less collapsed. The *b* cell parameter decreases less in H_2 than in He, Figure 2. Previously, in empty TON,[12] the pore collapse was found to result in a more important decrease in *b*.

Very important changes occur at around 5.5 GPa. This pressure is above the solidification point of the bulk hydrogen and weak single crystal reflections are observed as spots on the two-dimensional diffraction images on the detector corresponding to the hexagonal solid phase of H_2.[16] The superlattice peaks of TON disappear and the remaining peaks shift strongly to lower 2θ values, sharpen and the monoclinic splitting disappears. The structure of the framework can be readily refined using the $Cmc2_1$ space group, Figures S3, S4 and Table S14. The volume was found to be 22 % greater than the extrapolated volume of the collapsed $P2_1$ phase and in fact even 5 % higher than TON under ambient conditions in the $Cmc2_1$ structure. The most probable cause of this strong increase is an important increase in the H_2 content in the pores of TON swelling the structure. To our knowledge, such a major increase in unit cell volume due to guest insertion has never been observed in a zeolite. The 22 % volume increase is linked to a high degree of flexibility in the framework and results in symmetrization of the pores and the structure as a whole. The pore volume increases by 33 %, from 4.8 to 6.1 GPa, whereas the unit cell volume increases by 18 % between these two pressures. This contribution to the overall volume increase arising from the larger pore volume is 27 %, indicating that the remaining 73 % arises from the flexible framework, which has to adapt to the expansion of the pores by changes in Si–O–Si bond angles in various rings of tetrahedra in the framework. Overall, there is a general increase in the Si–O–Si angles in this process of expansion, Figure S4, Tables S10, S13 and S16. Hydrogen may also enter the small cages built up of 5- and 6-membered rings of SiO_4 tetrahedra in the framework. This symmetrization and swelling is stronger in *b* and *c*, which were the more compressible directions initially. At 6.1 GPa, the relative pore volume is 44 % greater than the interpolated pore volume of TON in He at the same pressure, Figure 2(c). This would also be consistent with a greater number of guests in H_2 than in He. Whereas a free rotating H_2 molecule is larger than a helium atom, a significant decrease in size would occur if free rotation is suppressed. This would allow additional H_2 molecules to enter the pores. This is supported by the decrease at 6.1 GPa in the relative intensity of the low angle diffraction lines, Figure 1, which is very sensitive to the guest content.

Normal compression of the higher symmetry structure is observed with further increases in pressure; however, the compressibility is 55 % lower than for the $P2_1$ phase with a lower H_2 content and 40 % lower than for He-filled TON in the same pressure range. The material also becomes increasingly strained with continuous broadening of the diffraction lines up to 35 GPa. The observed volume change is reversible on decompression and transformation to an orthorhombic $Pbn2_1$ phase is observed.

Raman spectroscopy (Figure 3) also provides insights into the filling of TON by H_2, as shown by spectra of the H_2 vibron for the TON/H_2 mixture measured on compression at two selected pressures below and above the $P2_1$-$Cmc2_1$ phase transition observed by XRD. These spectra are compared with the spectra of pure, bulk H_2, which were measured at sample locations without the TON powder and normalized to the same maximum intensity. From this comparison, it immediately appears that the spectra of the mixture are dominated by the strong peak of bulk H_2, which results from the pure hydrogen surrounding the TON crystallites. Additional weak features shifted to lower (higher) frequencies at 3.27 GPa (8.26 GPa) by a few tens of wavenumbers are present that are assigned to H_2 inserted into the pores and also, potentially, into the small cages of the zeolite. This assignment is simple since bulk hydrogen shows only a single strong peak, so there is indeed no reasonable origin for the additional weak shifted features other than vibrational modes arising from hydrogen molecules inserted in the zeolite due to the change in the local environment of these H_2 molecules. At 3.27 GPa in the $P2_1$ phase, the spectra show a broad, shapeless feature for inserted hydrogen, which is barely resolved from the main peak of bulk hydrogen and likely indicates positional disorder for the inserted molecules. On the other hand, two much better resolved and sharper peaks are seen at 8.26 GPa in the $Cmc2_1$ phase for inserted hydrogen, indicating the partial suppression of positional disorder and the appearance of a certain degree of orientational order. Furthermore, the hydrogen inserted in $Cmc2_1$ should occupy at least two nonequivalent sites of the same symmetry or even two sites of different symmetry, since we observe two distinct Raman peaks for the confined molecules.

Grand Canonical Monte Carlo simulations (see SI) were used to investigate the insertion of H_2 in the nanoporosity of TON using the experimental lattice parameters. As expected, the inserted amount of H_2 increases with increasing pressure, Figure 4 (a). Strikingly, these data show an important discontinuity between 3 and 6 GPa corresponding to an increase in the amount of H_2 by more than a factor of 3. As can be seen in the typical molecular configurations in Figure 4 (b) for two different pressures, this drastic change in the amount of inserted H_2 corresponds to additional insertion also within the small cages of the TON framework. While insertion at pressures below 3 GPa occurs exclusively in the pores, the significant insertion in the pores at higher pressures is a consequence of a swelling of the framework due to H_2 insertion in the small cages producing symmetrical uncollapsed pores. There thus appears to be a threshold

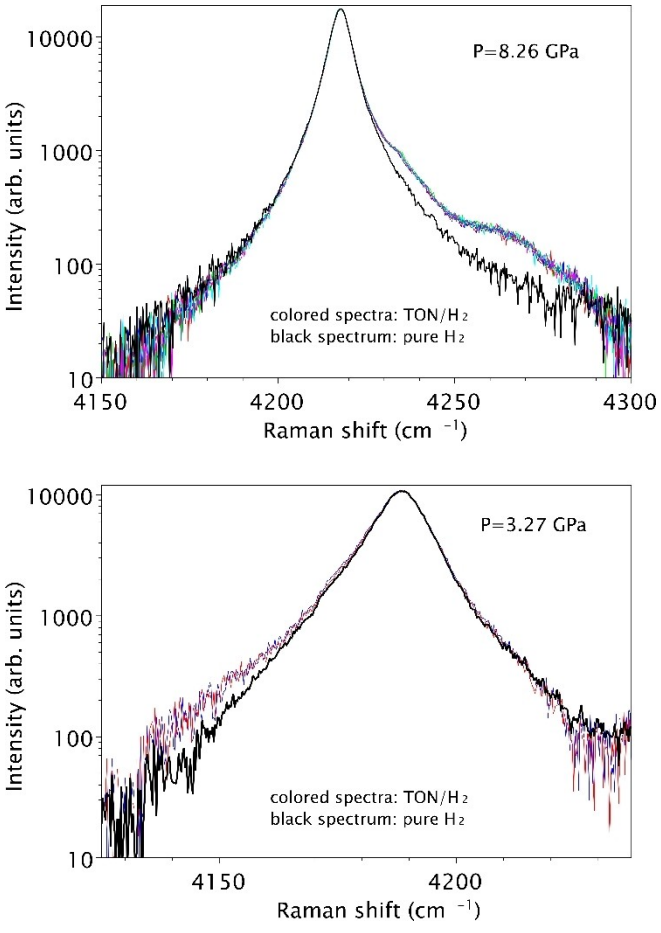

Figure 3. Raman spectra of the H_2 vibron measured on the TON/H_2 mixture, where both hydrogen-filled TON and bulk hydrogen are present (different colors for different points) and on pure H_2 (bold black), in the same sample, showing the contribution from inserted hydrogen in TON as an extra-intensity with respect to pure H_2. Spectra have been vertically rescaled to the same maximum intensity.

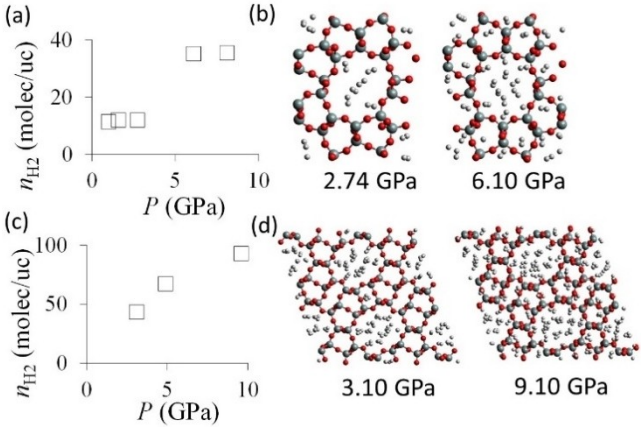

Figure 4. Simulated amount of inserted hydrogen (molecules/unit cell) as a function of pressure P in (a) TON and (c) MTW at room temperature. Typical molecular configurations generated using Monte Carlo modeling at different pressures for H_2 insertion in (b) TON at 2.74 and 6.10 GPa and (d) MTW at 3.10 and 9.10 GPa

pressure of about 5.5 GPa for the insertion of the linear H_2 molecules in these small cages. The much higher H_2 content in the pores results in a major increase in the pore diameter and a change to a more symmetrical pore shape yielding stronger increases in the *b* with respect to the *a* parameter as with the symmetrization of the structure the long pore now axis lies along *b* rather than along the diagonal of the unit cell. The *c* cell parameter corresponding to the pore axis also increases in a similar manner to *b*.

The hydrogen insertion behavior of 1D TON is very different from that observed for the zeolite MFI with a 3D pore system. In MFI, filling with He and H_2 is similar[5c,8] with reduced compression with respect to other guests and in the case of He a phase transition with a small positive volume change of close to 3 %, at about 10 GPa. The 1D structure of TON, formed by parallel zig-zag chains of six-membered rings, gives rise to greater flexibility of the framework permitting greater possibilities for swelling of the structure, which can behave in a similar manner to a wine rack. The 1D pore system may also be more favorable for the ordering of H_2 with the loss of rotational freedom rather than the complex 3D system of MFI with intersecting linear and sinusoidal pores with more potentially different environments.

In order to verify if such large volume increases due to hydrogen insertion could be a general characteristic of zeolites with 1D pores systems at high pressure, the MTW zeolite with larger 6.9 Å×5.6 Å pores, also formed by parallel zig-zag chains, was investigated by x-ray diffraction at high pressure, Figures 5, S5–S6 and Tables S17–S24. Two major changes were observed near 4.3 and 7.6 GPa on compression, Figure 5, with the shift of the diffraction lines towards low angles due to increases in the unit cell parameters. No change in the *C*2/*c* space group was observed. At these given pressures, there is a coexistence of two states with different hydrogen contents. Before the first change, the unit cell parameters and volume, Figure 5, were already much higher than in empty MTW.[13] They were also significantly higher than observed previously in argon-filled MTW,[13] indicating a much greater degree of filling with the H_2 molecules. The high-pressure phase transition to the collapsed *P*2/*n* structure observed in empty MTW[13] does not occur. At 4.3 GPa the *a* and *c* parameters increase returning to close to their values under ambient pressure and a strong increase is observed along the pore direction with an increase of the *b* parameter of close to 6 %, Figure 5 and Table S17. The monoclinic β angle continues to decrease monotonously. The overall volume increase is 11 % indicating a large increase in the quantity of hydrogen in the pores. This is also very clear from the larger pore diameters observed above 4.3 GPa, Figure S6, which are in fact similar to those observed at ambient pressure in empty MTW.

At 7.6 GPa, a very strong increase in the *a* parameter occurs with relatively little change in *b* and *c*. A strong increase in the monoclinic β angle occurs and this angle continues to increase with increasing pressure. The increase in *a* and in relative volume is of the order of 4 %. All cell parameters are much greater than those measured in non-penetrating DAPHNE oil under pressure. The strong

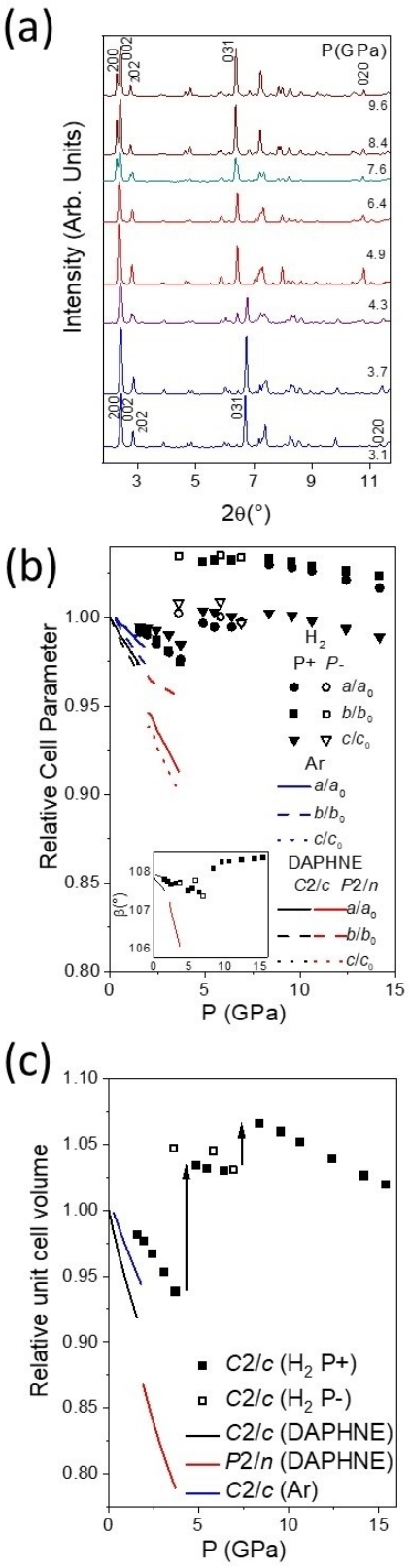

Figure 5. (a) X-ray diffraction patterns of MTW in hydrogen as a function of pressure (λ = 0.4828 Å). Selected reflections are indexed at 3.1 and 9.6 GPa. (b) Relative unit cell parameters and (c) relative unit cell volume of MTW in H_2 as a function of pressure. Error bars are smaller than the symbol size. Data for MTW in DAPHNE7474, and Ar are from previous work.[13] The monoclinic angle β for MTW in H_2 is given in the inset.

increase in *a* results in an elongation of the pores of the MTW structure. Again, Monte Carlo data were obtained, Figure 4(c), by considering the lattice parameters assessed experimentally. Similar to what is reported above for TON and illustrated using typical molecular configurations in Figure 4(d), H_2 insertion increases drastically with pressure and significant insertion occurs due to a densification of H_2 in the pores and H_2 insertion in the framework cages. H_2 insertion in the framework cages has a similar effect on the *a* and *c* unit cell parameters with a stronger increase being observed along the direction of the pore axis corresponding to the *b* parameter. This is followed by a change in pore shape with an alignment of the long pore axis along ***a*** giving rise to a strong increase in this cell parameter. The vast majority of intertetrahedral Si–O–Si angles increase due to swelling at the first positive volume jump followed by more complex changes with the modification in pore shape after the second volume increase, Figure S6, Tables S20, S23 and S26.

On decompression below 7.6 GPa, retransformation to the intermediate state is observed; however, this state persists to pressures lower than 4.3 GPa on pressure release indicating a degree of hysteresis and thus some metastablility for the form with the intermediate H_2 content.

Metastability is of interest for eventual hydrogen storage applications. Thus, the present study indicates that potentially metastable, hydrogen-filled zeolites can be obtained by high pressure insertion of H_2 both in the pores of the zeolite and, in contrast to other atoms and molecules, in the framework of the zeolite providing a mechanism for large volume expansion and strongly increased hydrogen capacity.

Supporting Information

The authors have cited additional references within the Supporting Information.[17,18,19,20,21,22,23,24,25,26,27]

Acknowledgements

We acknowledge DESY (Hamburg, Germany), a member of the Helmholtz Association HGF, for the provision of experimental facilities. Parts of this research were carried out at PETRA III using the P02.2 Extreme Conditions Beamline. Beamtime was allocated for proposals I-20190775EC and I-20220012EC. Calculations were performed using the Dahu platform of the GRICAD infrastructure (https://gricad.univ-grenoble-alpes.fr), which is supported by the Rhône-Alpes region (GRANT CPER07-13 CIRA) and the Equip@Meso project (reference ANR-10- EQPX-29- 01) of the programme Investissements d'Avenir supervised by the French Research Agency.

Conflict of Interest

The authors declare no conflict of interest.

Data Availability Statement

The data that support the findings of this study are available from the corresponding author upon reasonable request.

Keywords: hydrogen · zeolites · high-pressure · X-ray diffraction · Monte Carlo simulation

[1] W. Lubitz, W. Tumas, *Chem. Rev.* **2007**, *107*, 3900–3903.
[2] N. W. Ashcroft, *Phys. Rev. Lett.* **1968**, *21*, 1748–1749.
[3] W. J. Nellis, *Chem. Eur. J.* **1997**, *3*, 1921–1924.
[4] L. Schlapbach, A. Züttel, *Nature* **2001**, *414*, 353–358.
[5] a) V. P. Ting, A. J. Ramirez-Cuesta, N. Bimbo, J. E. Sharpe, A. Noguera-Diaz, V. Presser, S. Rudic, T. J. Mays, *ACS Nano* **2015**, *9*, 8249–8254; b) R. J. Olsen, A. K. Gillespie, C. I. Contescu, J. W. Taylor, P. Pfeifer, J. R. Morris, *ACS Nano* **2017**, *11*, 11617–11631; c) W. Xu, X. D. Liu, M. Pena-Alvarez, H. C. Jiang, P. Dalladay-Simpson, B. Coasne, J. Haines, E. Gregoryanz, M. Santoro, *J. Phys. Chem. C* **2021**, *125*, 7511–7517; d) M. Tian, M. J. Lennox, A. J. O'Malley, A. J. Porter, B. Kruner, S. Rudic, T. J. Mays, T. Duren, V. Presser, L. R. Terry, S. Rols, Y. N. Fang, Z. L. Dong, S. Rochat, V. P. Ting, *Carbon* **2021**, *173*, 968–979; e) L. R. Terry, S. Rols, M. Tian, I. da Silva, S. J. Bending, V. P. Ting, *Nanoscale* **2022**, *14*, 7250–7261.
[6] B. Coasne, J. Haines, C. Levelut, O. Cambon, M. Santoro, F. Gorelli, G. Garbarino, *Phys. Chem. Chem. Phys.* **2011**, *13*, 20096–20099.
[7] M. Santoro, V. Veremeienko, M. Polisi, R. Fantini, F. Alabarse, R. Arletti, S. Quatieri, V. Svitlyk, A. van der Lee, J. Rouquette, B. Alonso, F. Di Renzo, B. Coasne, J. Haines, *J. Phys. Chem. C* **2019**, *123*, 17432–17439.
[8] M. Santoro, W. W. Dong, K. Glazyrin, J. Haines, *J. Phys. Chem. C* **2021**, *125*, 24249–24253.
[9] D. Paliwoda, D. Comboni, T. Poreba, M. Hanfland, F. Alabarse, D. Maurin, T. Michel, U. B. Demirci, J. Rouquette, F. di Renzo, A. van der Lee, S. Bernard, J. Haines, *J. Phys. Chem. Lett.* **2021**, *12*, 5059–5063.
[10] J. M. Thibaud, J. Rouquette, K. Dziubek, F. A. Gorelli, M. Santoro, G. Garbarino, S. Clement, O. Cambon, A. van der Lee, F. Di Renzo, B. Coasne, J. Haines, *J. Phys. Chem. C* **2018**, *122*, 8455–8460.
[11] M. Santoro, M. Morana, D. Scelta, J. Rouquette, K. Dziubek, F. A. Gorelli, R. Bini, G. Garbarino, A. van der Lee, F. Di Renzo, B. Coasne, J. Haines, *J. Phys. Chem. C* **2021**, *125*, 19517–19524.
[12] J. M. Thibaud, J. Rouquette, P. Hermet, K. Dziubek, F. A. Gorelli, M. Santoro, G. Garbarino, F. G. Alabarse, O. Cambon, F. Di Renzo, A. van der Lee, J. Haines, *J. Phys. Chem. C* **2017**, *121*, 4283–4292.
[13] D. Paliwoda, M. Fabbiani, F. Alabarse, P. Hermet, J. Rouquette, F. Di Renzo, J. Haines, *J. Phys. Chem. C* **2022**, *126*, 2877–2884.
[14] D. W. Breck, *Zeolite Molecular Sieves: Structure, Chemistry and Use.*, John Wiley & Sons, Inc, New York, **1974**.
[15] a) H. Shimizu, E. M. Brody, H. K. Mao, P. M. Bell, *Phys. Rev. Lett.* **1981**, *47*, 128–131; b) A. Polian, M. Grimsditch, *Europhys. Lett.* **1986**, *2*, 849–855.
[16] H. K. Mao, A. P. Jephcoat, R. J. Hemley, L. W. Finger, C. S. Zha, R. M. Hazen, D. E. Cox, *Science* **1988**, *239*, 1131–1134.
[17] F. Di Renzo, F. Remoue, P. Massiani, F. Fajula, F. Figueras, T. Descourieres, *Zeolites* **1991**, *11*, 539–548.
[18] F. Di Renzo, F. Remoue, P. Massiani, F. Fajula, F. Figueras, *Thermochim. Acta* **1988**, *135*, 359–364.
[19] H. K. Mao, J. Xu, P. M. Bell, *J. Geophys. Res.* **1986**, *91*, 4673–4676.

[20] G. Shen, Y. Wang, A. Dewaele, C. Wu, D. E. Fratanduono, J. Eggert, S. Klotz, K. F. Dziubek, P. Loubeyre, O. V. Fat′yanov, P. D. Asimow, T. Mashimo, R. M. M. Wentzcovitch, J. Bass, Y. Bi, D. He, K. V. Khishchenko, K. Leinenweber, B. Li, T. Sakai, T. Tsuchiya, K. Shimizu, D. Yamazaki, M. Mezouar, I. T. Grp, *High Pressure Res.* **2020**, *40*, 299–314.
[21] H. P. Liermann, Z. Konopkova, W. Morgenroth, K. Glazyrin, J. Bednarcik, E. E. McBride, S. Petitgirard, J. T. Delitz, M. Wendt, Y. Bican, A. Ehnes, I. Schwark, A. Rothkirch, M. Tischer, J. Heuer, H. Schulte-Schrepping, T. Kracht, H. Franz, *J. Synchrotron Radiat.* **2015**, *22*, 908–924.
[22] C. Prescher, V. B. Prakapenka, *High Pressure Res.* **2015**, *35*, 223–230.
[23] Deposition Numbers 2355549 (for TON/H_2 1.0 GPa), 2355550 (for TON/H_2 2.7 GPa), 2355551 (for TON/H_2 8.1 GPa), 2355552 (for TON/He 0.3 GPa), 2355553 (for TON/He 2.9 GPa), 2355554 (for MTW/H_2 3.1 GPa), 2355555 (for MTW/H_2 9.6 GPa) and 2355556 (for MTW/H_2 4.9 GPa), contain the supplementary crystallographic data for this paper. These data are provided free of charge by the joint Cambridge Crystallographic Data Centre and Fachinformationszentrum Karlsruhe Access Structures service Access Structures service.
[24] J. Rodriguez-Carvajal, *Appl. Crystallogr.* **2001**, 30–36.
[25] K. Momma, F. Izumi, *J. Appl. Crystallogr.* **2011**, *44*, 1272–1276.
[26] F. Darkrim, D. Levesque, *J. Chem. Phys.* **1998**, *109*, 4981–4984.
[27] N. Desbiens, I. Demachy, A. H. Fuchs, H. Kirsch-Rodeschini, M. Soulard, J. Patarin, *Angew. Chem. Int. Ed.* **2005**, *44*, 5310–5313.

Manuscript received: April 5, 2024
Accepted manuscript online: May 15, 2024
Version of record online: ■■, ■■

Communications

Hydrogen Storage

M. Santoro, J. Rouquette, M. Fabbiani, F. di Renzo, B. Coasne, W. Dong, K. Glazyrin, J. Haines* ——— **e202406425**

Strong Swelling and Symmetrization in Siliceous Zeolites due to Hydrogen Insertion at High Pressure

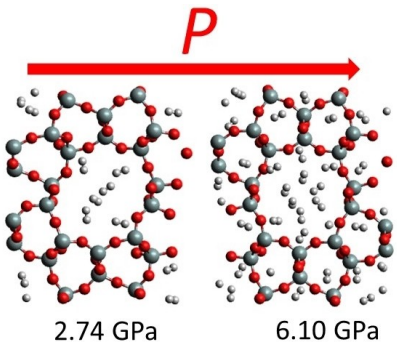

In contrast to other atoms or molecules, H_2 enters both the pores and the framework cages of siliceous zeolites under high pressure. This results in strong swelling and symmetrization of the structures with very high hydrogen contents of 1.5–1.7 H_2 molecules/SiO_2 unit being obtained.